A Riemannian Scalar Measure for Diffusion Tensor Images

Andrea Fuster[1], Laura Astola[2], and Luc Florack[2]

[1] Department of Biomedical Engineering, Eindhoven University of Technology, The Netherlands
a.fuster@tue.nl
[2] Department of Mathematics and Computer Science, Eindhoven University of Technology, The Netherlands
l.j.astola@tue.nl, l.m.j.florack@tue.nl

Abstract. We study a well-known scalar quantity in differential geometry, the Ricci scalar, in the context of Diffusion Tensor Imaging (DTI). We explore the relation between the Ricci scalar and the two most popular scalar measures in DTI: Mean Diffusivity and Fractional Anisotropy. We discuss results of computing the Ricci scalar on synthetic as well as real DTI data.

1 Introduction

Diffusion Tensor Imaging (DTI) is a magnetic resonance imaging technique that measures diffusion of water molecules in tissue in a non-invasive way [1,2,3]. It is mostly used for the study of brain white matter. DTI is used in clinical research e.g. for localization of brain tumors in relation to white matter tracts, assisting in surgical planning and in the assessment of white matter maturation in children. Information about the white matter architecture and integrity can be extracted from the so-called diffusion tensor.

Different scalar measures (scalar quantities constructed from the diffusion tensor) have been proposed in the literature, aiming to reveal information about the underlying diffusion process and tissue structure. Scalar measures are also studied to relate the state of white matter to different pathologies. The most common ones are the mean diffusivity (MD) and fractional anisotropy (FA) [4].

Mean diffusivity can be interpreted as average diffusion per imaged voxel. In general, MD is smaller in areas with organized tissue. This allows mean diffusivity images to show main white matter tracts but no detailed structure. Fractional anisotropy measures the anisotropy of the diffusion. Roughly speaking, there is more diffusion along elongated structures than across them. High FA values typically indicate the presence of such an elongated structure while low values relate to isotropic diffusion and scarcity or absence of structures. However, low FA values are also found in voxels with complicated fiber architecture such as crossings [5]. Both MD and FA give relevant information about white matter but have limitations as well. It is therefore also worth to study other scalar DTI measures which could improve the clinical utility of DTI.

X. Jiang and N. Petkov (Eds.): CAIP 2009, LNCS 5702, pp. 419–426, 2009.

In this paper we consider a well-known scalar quantity in differential geometry, the Ricci scalar, in the context of DTI. The Ricci scalar has been used in 2D image processing for curvature analysis [6]. The goal of this research is to evaluate whether the Ricci scalar can provide additional information on white matter structures w.r.t. the usual scalar measures. We found promising preliminary results on simulated and phantom data showing high negative values of the Ricci scalar at voxels with crossing structures.

2 Theory

In the DTI model diffusion is represented by the diffusion tensor D. This is a symmetric, positive definite second-order tensor in dimension three constructed from the DTI measurements. On the other hand, a metric tensor g (see, for example, [7]) is a second-order symmetric positive definite tensor field on a manifold which defines the inner product of two tangent vectors v, w as

$$\langle v, w \rangle = g_{ij} v^i w^j \tag{1}$$

The relation between a Riemannian metric and its inverse is[1]

$$g_{ik} g^{kj} = \delta_i^j \tag{2}$$

The diffusion tensor can naturally be associated to (the inverse of) a Riemannian metric tensor in dimension three [8]:

$$D^{ij} = g^{ij}, \quad i, j = 1, 2, 3 \tag{3}$$

In this way large diffusion in a certain direction corresponds to a short distance in the metric space. A number of authors have studied DTI in the Riemannian framework [9,10,11,12].

Different scalar quantities can be constructed from contractions of the metric and its curvature tensors. The simplest of those is the so-called Ricci scalar, intrinsically related to the geometry of the metric space. The Ricci scalar is given by (see, for example, [13]):

$$R = g^{ij} R_{ij} \tag{4}$$

where R_{ij} is the Ricci curvature tensor (see Appendix). Unlike the metric, the Ricci tensor is not positive definite, allowing for both positive and negative values of the Ricci scalar. This is a major difference with respect to the usual DTI scalar measures, which are always positive. In fact, the Ricci scalar in dimension two is twice the Gaussian curvature. For example, the Ricci scalar on a unit sphere is a positive quantity: $R = 2$. On the other hand, on a saddle surface the Ricci scalar is negative everywhere (except at the origin). In dimension three the Ricci scalar does not completely characterize the curvature but represents instead the average of the characterizing curvatures.

[1] In this paper we use Einstein's summation convention, $a_i a^i = \sum_i a_i a^i$.

2.1 Ricci Scalar and Mean Diffusivity

The Ricci scalar is related to the mean diffusivity (MD):

$$\mathrm{MD} = \frac{1}{3}(\lambda^1 + \lambda^2 + \lambda^3) \tag{5}$$

where the λ's are the eigenvalues of the diffusion tensor. Indeed, we can write:

$$R = g^{ij}R_{ij} \overset{(3)}{=} D^{ij}R_{ij} = \tilde{D}^{ij}\tilde{R}_{ij} = \lambda^1\tilde{R}_{11} + \lambda^2\tilde{R}_{22} + \lambda^3\tilde{R}_{33} \tag{6}$$

The last two equalities follow from the fact that R is a scalar quantity and thus independent of the used coordinate system; we choose the coordinate system in which the diffusion tensor is diagonal, and denote tensors in this coordinate system with a tilde. Comparing (6) to (5) it is clear that we can think of the Ricci scalar as a kind of curvature-weighted mean diffusivity.

2.2 Ricci Scalar and Fractional Anisotropy

The Ricci scalar is intrinsically different from the fractional anisotropy in the following sense. A zero FA value indicates (perfect) isotropic diffusion (see Fig. 1 top left) while a non-zero value indicates anisotropy to some degree, i.e., the presence of structures obstructing the diffusion process. On the other hand, a zero Ricci scalar can indicate both isotropy or anisotropy (see Fig. 1 top left and right). The same is true for a non-zero Ricci scalar (see Fig. 1 bottom left and right).

More precisely, a homogeneous isotropic diffusion corresponds to the case where

$$\lambda^1 = \lambda^2 = \lambda^3 = \lambda \tag{7}$$

In this case the fractional anisotropy

$$\mathrm{FA} = \frac{\sqrt{3}}{\sqrt{2}}\frac{\sqrt{(\lambda^1 - \mathrm{MD})^2 + (\lambda^2 - \mathrm{MD})^2 + (\lambda^3 - \mathrm{MD})^2}}{\sqrt{(\lambda^1)^2 + (\lambda^2)^2 + (\lambda^3)^2}} \tag{8}$$

is just zero. The Riemannian metric and inverse metric associated to the isotropic diffusion tensor are Euclidean:

$$g_{ij} = \frac{1}{\lambda}\begin{pmatrix} 1 & 0 & 0 \\ 0 & 1 & 0 \\ 0 & 0 & 1 \end{pmatrix}, \quad g^{ij} = \lambda\begin{pmatrix} 1 & 0 & 0 \\ 0 & 1 & 0 \\ 0 & 0 & 1 \end{pmatrix} \tag{9}$$

The Riemann tensor of a Euclidean metric is zero. It is clear from equation (10) that the Ricci tensor will also be zero, and so will be the Ricci scalar. In this way we have shown that homogeneous isotropic diffusion implies a zero Ricci scalar. However, this is not the only case where the Ricci scalar is zero. Another situation in which this happens is when the diffusion tensor field is homogeneous and anisotropic. Note that FA in this case would be different from zero.

We conclude that the Ricci scalar and fractional anisotropy certainly have a different character. The zeros (non-zeros) of the Ricci scalar cannot be always related to isotropic (anisotropic) diffusion as in the case of FA.

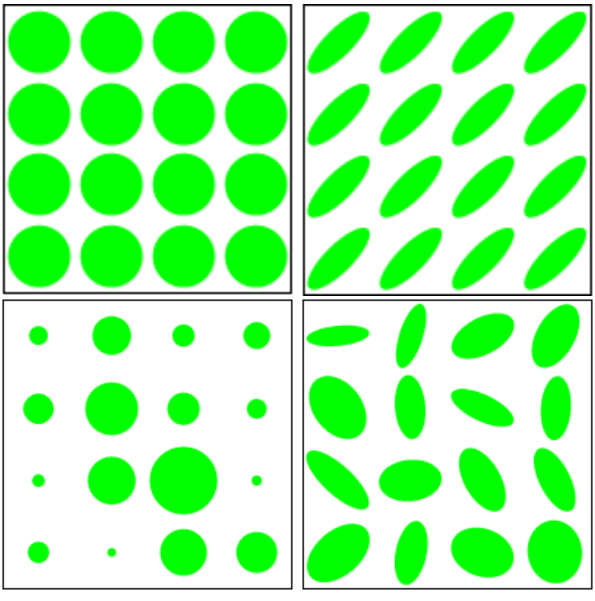

Fig. 1. Top left: Homogeneous isotropic tensor field: $R = \text{FA} = 0$. Top right: Homogeneous anisotropic case: $R = 0,\ \text{FA} \neq 0$. Bottom left: Inhomogeneous isotropic case: $R \neq 0,\ \text{FA} = 0$. Bottom right: Inhomogeneous anisotropic case: $R \neq 0,\ \text{FA} \neq 0$.

3 Experiments

In order to explore the geometric significance of the Ricci scalar, we have experimented with simulated, phantom and real data.

Simulated Data

To get a quick insight in what the Ricci scalar can detect in a tensor field, we refer to Fig. 2, where we have simulated a crossing of orthogonally oriented sets of tensors, modeling homogeneous diffusion tensors corresponding to two fiber bundles. The voxels where the Ricci scalar is non-zero are colored according to its sign. In the crossing region of this tensor field, the Ricci scalar tends to be large and negative. Since the Ricci scalar involves second order derivatives (see Appendix), the minimum size of the region to be considered depends on the scale of the Gaussian differential operator [14] [15] [16].

Phantom Data

We computed Ricci scalars on a real phantom data consisting of cylinder containing a water solution, three sets of crossing synthetic fiber bundles and three supporting pillars on the boundary. In Fig. 3 we see that in the region where the fiber bundles cross Ricci scalars have relatively large negative values, despite

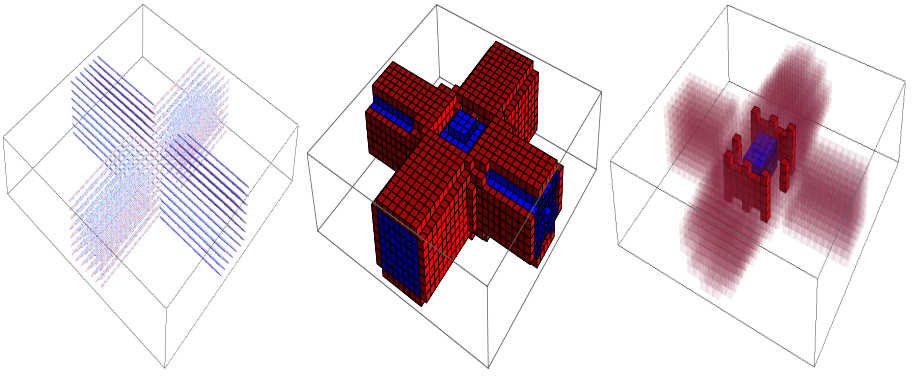

Fig. 2. Left: A simulated crossing of tensors. Middle: Ricci scalars computed on the tensor field, blue for negative- and red for positive values. Right: Voxels where the absolute value of Ricci scalar is the highest.

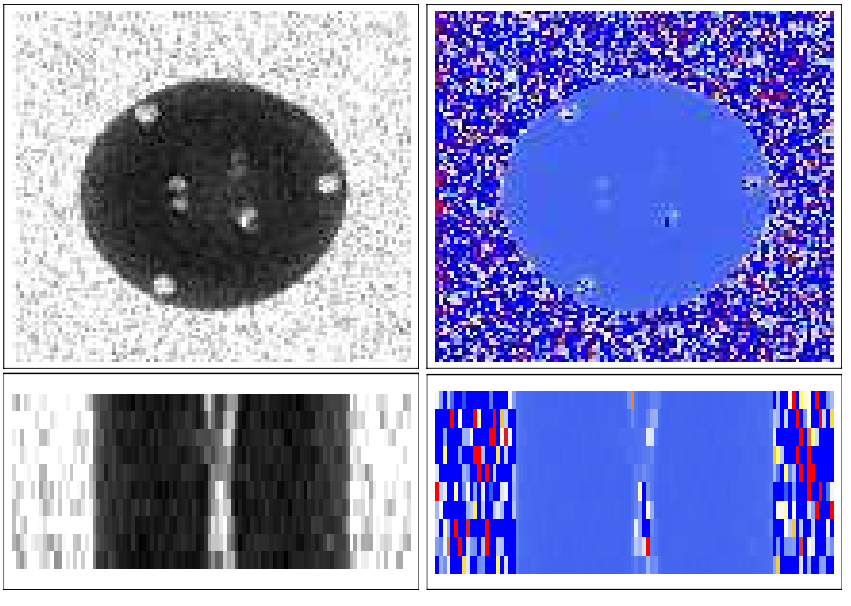

Fig. 3. Top left: Mean diffusivity on a trans-axial slice of the cylinder. Top right: A temperature map of Ricci scalars on the same slice. Blue indicates negative values. Bottom left: Mean diffusivity on an axial slice containing crossing fiber bundles. Bottom right: Ricci scalars on the same slice. Large negative values found in the crossing.

of the noisy nature of the DTI-data. This might be explained by the fact that crossings can be related to saddle shaped structures [17], for which the Ricci scalar has a negative value.

Real Data

We have also experimented with real DTI data of a rat brain. We plotted the Ricci scalars in a temperature map, to emphasize the differences in sign. We identified positive (negative) outliers of the Ricci scalar data with maximum (minimum) values of the rest of the data. The Ricci scalar gives information about the variations in diffusion tensor orientations unlike FA, which will identify tensors with similar anisotropy even though their orientation may differ. This can be seen e.g. in the boxed region in Fig. 4, which is known to have complex structure [18].

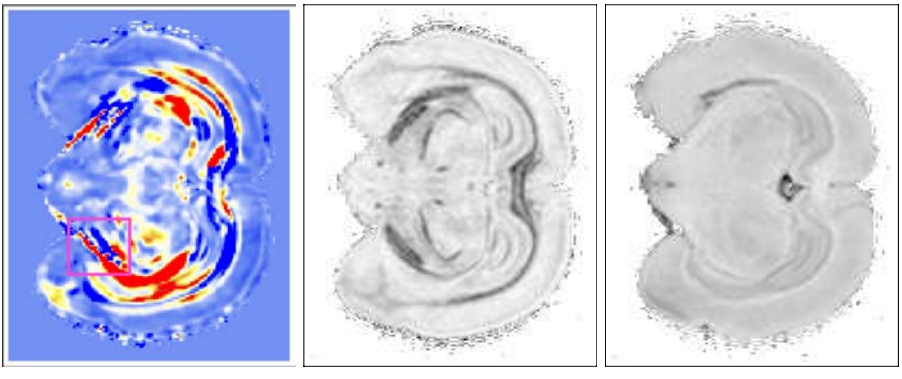

Fig. 4. Left: Ricci scalars on a slice of the rat brain DTI image. Middle: Fractional anisotropy. Right: Mean diffusivity.

4 Discussion

The Ricci scalar on real DTI images show rough structures in a similar way to FA and MD. The more complex curvature related information cannot be fully appreciated with a 2D visualization, since both the Ricci scalar and DTI data are intrinsically 3D. Work in progress includes the integration of the Ricci scalar into a 3D DTI visualization toolkit, which can also render the so-called high angular resolution diffusion images (HARDI) [19]. The simulated and phantom data images show large negative values of the Ricci scalar at fiber crossings. The theoretical explanation for this fact should be refined. Therefore, more work is needed to investigate whether the Ricci scalar can be used in the detection of fiber crossings in DTI data. If this indeed is the case, besides in fiber tracking it would be helpful for voxel classification [20], where the regions with single orientation could be identified as the regular DTI data (second order tensors), and higher order models (e.g. fourth order tensors) could be used in regions where inhomogeneous fiber population is anticipated. It could also be useful in the so-called splitting tracking method in HARDI framework [21], by indicating the potential bifurcation points of fiber bundles with large negative values.

Acknowledgements

L. Astola and L. Florack gratefully acknowledge The Netherlands Organization for Scientific Research (NWO) for financial support. We also want to thank Ellen Brunenberg at Eindhoven University of Technology for providing the rat HARDI data and Pim Pullens at Maastricht University for providing the phantom HARDI data.

References

1. Basser, P., Mattiello, J., Turner, R., Le Bihan, D.: Diffusion tensor echo-planar imaging of human brain. In: Proceedings of the SMRM, p. 584 (1993)
2. Basser, P.J., Mattiello, J., Lebihan, D.: Estimation of the effective self-diffusion tensor from the NMR spin echo. Journal of Magnetic Resonance Series B 103, 247–254 (1994)
3. Basser, P.J., Mattiello, J., Lebihan, D.: MR diffusion tensor spectroscopy and imaging. Biophysical Journal 66, 259–267 (1994)
4. Basser, P., Pierpaoli, C.: Microstructural and physiological features of tissues elucidated by quantitative-diffusion-tensor MRI. Journal of Magnetic Resonance. Series B 111(3), 209–219 (1996)
5. Özarslan, E., Vemuri, B.C., Mareci, T.H.: Generalized scalar measures for diffusion MRI using trace, variance, and entropy. Magn. Reson. Med. 53(4), 866–876 (2005)
6. Saucan, E., Appleboim, E., Wolanski, G., Zeevi, Y.: Combinatorial ricci curvature for image processing. Presented at MICCAI 2008 Workshop Manifolds in Medical Imaging: Metrics, Learning and Beyond (2008)
7. Nakahara, M.: Geometry, Topology and Physics, 2nd edn. Graduate Student Series in Physics. Taylor & Francis, Abington (2003)
8. de Lara, M.C.: Geometric and symmetry properties of a nondegenerate diffusion process. The Annals of Probability 23(4), 1557–1604 (1995)
9. O'Donnell, L., Haker, S., Westin, C.-F.: New approaches to estimation of white matter connectivity in diffusion tensor MRI: Elliptic pDEs and geodesics in a tensor-warped space. In: Dohi, T., Kikinis, R. (eds.) MICCAI 2002. LNCS, vol. 2488, pp. 459–466. Springer, Heidelberg (2002)
10. Lenglet, C., Deriche, R., Faugeras, O.: Inferring white matter geometry from diffusion tensor MRI: Application to connectivity mapping. In: Pajdla, T., Matas, J.G. (eds.) ECCV 2004. LNCS, vol. 3024, pp. 127–140. Springer, Heidelberg (2004)
11. Prados, E., Lenglet, C., Pons, J.P., Wotawa, N., Deriche, R., Faugeras, O., Soatto, S.: Control theory and fast marching techniques for brain connectivity mapping. In: Proceedings of the IEEE Conference on Computer Vision and Pattern Recognition, vol. 1, pp. 1076–1083. IEEE, New York (2006)
12. Astola, L., Florack, L.M.J., ter Haar Romeny, B.M.: Measures for pathway analysis in brain white matter using diffusion tensor images. In: Karssemeijer, N., Lelieveldt, B. (eds.) IPMI 2007. LNCS, vol. 4584, pp. 642–649. Springer, Heidelberg (2007)
13. Carroll, S.: Spacetime and Geometry: An Introduction to General Relativity. Addison-Wesley, Reading (2003)
14. Florack, L., Astola, L.: A multi-resolution framework for diffusion tensor images. In: CVPR Workshop on Tensors in Image Processing and Computer Vision, Anchorage, Alaska, The United States. CVPR, vol. 20, Springer, Heidelberg (2008)

15. ter Haar Romeny, B.M.: Front-End Vision and Multi-Scale Image Analysis: Multi-Scale Computer Vision Theory and Applications, written in Mathematica, vol. 27. Kluwer Academic Publisher, Dordrecht (2003)
16. Florack, L.M.J.: Image Structure, vol. 10. Kluwer Academic Publisher, Dordrecht (1997)
17. Faas, F., Van Vliet, L.: A crossing detector based on the structure tensor. In: Blanc-Talon, J., Philips, W., Popescu, D., Scheunders, P. (eds.) ACIVS 2007. LNCS, vol. 4678, pp. 212–220. Springer, Heidelberg (2007)
18. Brunenberg, E., Prckovska, V., Platel, B., Strijkers, G., ter Haar Romeny, B.M.: Untangling a fiber bundle knot: Preliminary results on STN connectivity using DTI and HARDI on rat brains. In: Proceedings of the 17th Meeting of the International Society for Magnetic Resonance in Medicine (ISMRM), Honolulu, Hawaii (2009)
19. Tuch, D., Reese, T., Wiegell, M., Makris, N., Belliveau, J., Wedeen, V.: High angular resolution diffusion imaging reveals intravoxel white matter fiber heterogeneity. Magnetic Resonance in Medicine 48(4), 577–582 (2002)
20. Alexander, D., Barker, G., Arridge, S.: Detection and modeling of non-gaussian apparent diffusion coefficient profiles in human brain data. Magnetic Resonance in Medicine 48, 331–340 (2002)
21. Deriche, R., Descoteaux, M.: Splitting tracking through crossing fibers: Multidirectional Q-ball tracking. In: Proceedings of the 4th International Symposium on Biomedical Imaging: From Nano to Macro (ISBI 2007), Arlington, Virginia, USA (2007)

Appendix

The Ricci tensor is a symmetric second-order tensor given by:

$$R_{ij} = R^{k}{}_{ikj} = \frac{\partial \Gamma^{k}_{ij}}{\partial x^{k}} - \frac{\partial \Gamma^{k}_{ik}}{\partial x^{j}} + \Gamma^{k}_{kl}\Gamma^{l}_{ij} - \Gamma^{k}_{jl}\Gamma^{l}_{ik} \tag{10}$$

where $R^{i}{}_{jkl}$ is the Riemann tensor and the Γ's are the Christoffel symbols:

$$\Gamma^{i}_{jk} = \frac{1}{2} g^{il}(\partial_k g_{lj} + \partial_j g_{lk} - \partial_l g_{jk}) \tag{11}$$